NANO LETTERS

Letter

pubs.acs.org/NanoLett

Optical Impedance Transformer for Transparent Conducting Electrodes

Ken Xingze Wang,[†,‡] Jessica R. Piper,[‡] and Shanhui Fan*[,‡]

[†]Department of Applied Physics and [‡]Department of Electrical Engineering, Stanford University, Stanford, California 94305, United States

ABSTRACT: A fundamental limitation of transparent conducting electrode design is thought to be the trade-off between photonic and electronic performances. The photonic transmission property of a transparent conducting electrode, however, is not intrinsic but depends critically on the electromagnetic environment where the electrode is located. We develop the concept of optical impedance transformation, and use this concept to design nanophotonic structures that provide broadband and omnidirectional reduction of optical loss in an ultrathin transparent conducting electrode, without compromising its electrical performance.

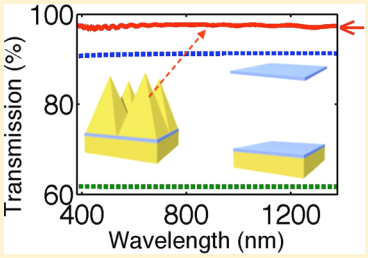

KEYWORDS: *Optical impedance transformer, photon management, solar cells, transparent conducting electrodes, nanopyramid, graphene*

Transparent conducting electrodes are important components in a variety of optoelectronic devices such as solar cells,[1] light-emitting diodes,[2] touch screens,[3] and smart windows.[4] A fundamental limitation of transparent conducting electrode design is thought to be the trade-off between photonic and electrical performances:[5−9] To achieve high optical transmission, one typically would reduce the material optical loss by, for example, reducing the carrier density, which then leads to lower electrical conductivity. We note, however, that the transmission property of a transparent conducting electrode is not intrinsic, but rather depends critically on the electromagnetic environment where the electrode is located. In this Letter, we develop the concept of optical impedance transformation and use this concept to design nanophotonic structures that provide broadband and omnidirectional reduction of optical loss in an ultrathin transparent conducting electrode, without compromising its electrical performance.

To illustrate the role of optical impedance in transparent electrode design we consider a transparent conducting electrode with thickness much smaller than the wavelength of interest,[10,11] which is embedded in a surrounding lossless electromagnetic environment characterized by electrical permittivity ε and magnetic permeability μ. As a starting point, we assume normally incident light. In the optical frequency range, the transparent conducting electrode itself is characterized by an optical conductivity σ. The time-averaged power loss per unit area of the electrode is then

$$p = \frac{1}{2}\sigma|\mathbf{E}|^2 d \tag{1}$$

where d is the thickness of the electrode and $\mathbf{E}$ is the complex amplitude of the electric field at the position of the transparent conducting electrode. As the lowest order approximation, if the reflection at the electrode region can be ignored, which is true, for example, for an ultrathin transparent conducting electrode made of graphene, the optical electric field $\mathbf{E}$ seen by the electrode can then be related to the optical power flux density S passing through the electrode by

$$S = \frac{|\mathbf{E}|^2}{2Z} \tag{2}$$

where

$$Z = \sqrt{\frac{\mu}{\varepsilon}} \tag{3}$$

is the impedance of the surrounding environment. Combining eqs 1 to 3, the power loss in the transparent electrode is related to the incident flux density by

$$p = \sigma d S Z \tag{4}$$

Therefore, for the same incident flux density S, reducing the impedance Z of the surrounding medium results in the reduction of the optical electric field that the transparent conducting electrode sees and hence the reduction of its optical loss.

It is therefore beneficial to surround the electrode with a high-index dielectric material, which has a low optical impedance. However, in typical optoelectronic devices using transparent electrodes light is incident from air. A flat interface between the high-index dielectric material and air would result in substantial reflection. Therefore, we consider the structure shown in Figure 1, where a nanopyramid array is placed at the interface between the high-index dielectric region and air as an antireflection strategy. The use of nanopyramids for antireflection is certainly well-known.[12−14] We emphasize in the

Received: February 26, 2014
Revised: April 22, 2014
Published: April 28, 2014

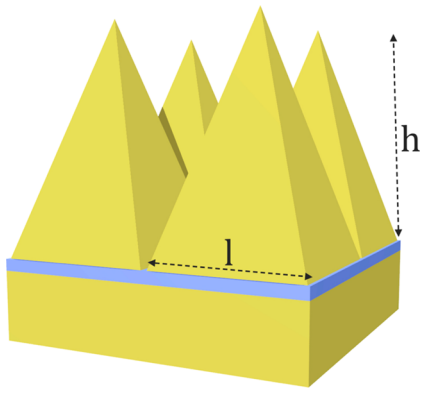

Figure 1. Graphene electrode with N graphene layers sandwiched between a flat substrate, which is assumed to be semi-infinite, and a nanostructured superstrate, which is a square lattice of nanopyramids. l is the base length and h is the height of a nanopyramid, and the lattice constant is equal to l. The material in blue represents graphene, and the material in yellow represents the surrounding lossless dielectric medium with a real refractive index of n.

present case, however, that the combination of the nanopyramid and the high-index dielectric medium surrounding the transparent electrode accomplishes an optical impedance transformation, through which one can reduce the optical loss of the transparent conducting electrode without sacrificing its electrical performance. Below we will refer to the structure in Figure 1, including both the nanopyramids above the electrode as the superstrate and the uniform media below the electrode as the substrate, as an optical impedance transformer.

In the following, we choose graphene as the transparent conducting electrode layer to demonstrate the optical impedance transformation concept. Graphene possesses many desirable mechanical, thermal, and chemical properties in addition to its high transparency and good conductivity.[15−19] A graphene monolayer absorbs $\pi\alpha \approx 2.3\%$ of the incoming light in the visible range, where α is the fine structure constant, and N layers of graphene absorb $N\pi\alpha$ of the incoming light.[20,21] These values, however, are only valid for bare graphene sheets suspended in air or vacuum.

We consider the transmission and absorption properties of the structure shown in Figure 1 with graphene embedded in it. We assume that the material of the surrounding media, that is, the substrate and the superstrate, has a real refractive index of $n = (\varepsilon/\varepsilon_0)^{1/2}$. Analytically, one expects that the absorption coefficient in each graphene layer is $\pi\alpha/n$ because the optical electric field intensity is reduced by a factor of n with the same optical flux density, according to eq 4. Similarly, a structure consisting of N-layer graphene electrode embedded in the optical impedance transformer has the following absorption and transmission coefficients

$$A = \pi\alpha\frac{N}{n} \tag{5}$$

$$T = 1 - \pi\alpha\frac{N}{n} \tag{6}$$

because we assume that the reflection is eliminated by the nanopyramids.

We compare the analytic results above, that is, eqs 5 and 6, against first-principles full-field electromagnetic simulations. The simulations use the optical constants of graphene layers in the visible and near-infrared ranges[22] and are based on the rigorous coupled-wave analysis.[23] In Figure 1, the thickness of the 4-layer graphene is 1.36 nm.[3,22] We first assume that the refractive index $n = 4$ for the surrounding medium, and that the substrate is semi-infinite due to its much greater thickness compared to the graphene electrode. A square lattice of pyramids made of the same dielectric material as the substrate is introduced onto the 4-layer graphene with the lattice constant being 120 nm and equal to the base length l, and the height $h = 1200$ nm. These l and h values are chosen purely based on intuitive arguments in ref 14. In general, to achieve effective antireflection the periodicity l needs to be in the subwavelength scale and the height h of the pyramids needs to be sufficiently large to provide an adiabatic impedance variation in the vertical direction. In addition, the periodicity l needs to be subwavelength to avoid exciting resonant modes for light trapping.

In Figure 2, the red curves show the absorption and transmission spectra of the structure of Figure 1 for light

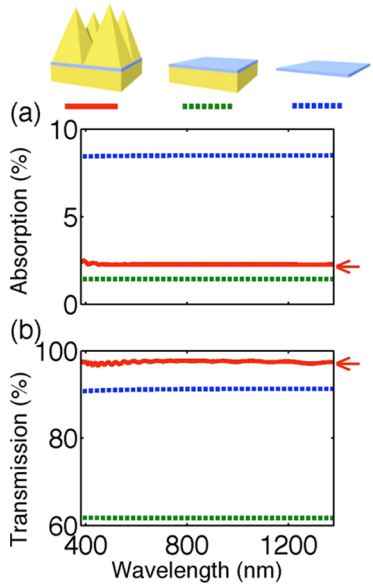

Figure 2. Comparison of (a) absorption and (b) transmission spectra at normal incidence for different structures shown at the top of the figure. The blue region represents a graphene electrode with $N = 4$ layers, and the yellow region represents the lossless substrates and superstrate with a refractive index of $n = 4$. The structures are placed in air except that the substrates are assumed to be semi-infinite. For the nanostructured superstrate, $l = 120$ nm and $h = 1200$ nm, where l and h are defined in Figure 1. The blue curves correspond to the bare graphene layers, the green curves correspond to the graphene layers on the substrate, and the red curves correspond to the structure with optical impedance transformation. The red left arrows to the right of the plots are theoretical predications by eqs 5 and 6

normally incident upon the structure. We see that both the absorption A and transmission T the of the structure are nearly independent of wavelength. Also, the reflection (as determined by $1 - A - T$) is nearly zero. Both the flatness of the spectra and the lack of reflection indicate the effectiveness of antireflection provided by the nanopyramids. The absorption and transmission coefficients agree very well with eqs 5 and 6. Thus, these simple formulas in fact are quite sufficient to capture the optical properties of the relatively complicated structure of Figure 1.

dx.doi.org/10.1021/nl500741f | Nano Lett. 2014, 14, 2755−2758

The structure in Figure 1 provides significantly enhanced transmission at T = 97.4% averaged over the entire visible wavelength range from 380 to 750 nm, as compared to the same graphene layers in air with an average T = 91% (blue curve in Figure 2b). The structure also provides significant suppression of absorption at A = 2.3%, as compared with the same graphene layers in air with A = 8.5%. The impedance transformation concept, as embodied in the structure of Figure 1, allows us to reduce the absorption of an ultrathin transparent conducting electrode without affecting its dielectric or conductive properties. Therefore, we have shown that the concept of optical impedance transformation allows us to bypass the typical trade-off in terms of optical transparency and electrical conductance.

We also compare the structure of Figure 1 with a more typical configuration where the graphene transparent electrode is placed on top of a high index substrate,[1,15,24] without the nanopyramids as a superstrate. The absorption and transmission spectra are plotted as green curves in Figure 2. Absorption in graphene is suppressed in this case but at the expense of high reflection. The absorption suppression here is due to the reflected wave being out of phase with the incident wave at the surface of the substrate, causing a local suppression of the electric field. Therefore, although the absorption coefficient in each graphene layer is $\pi\alpha[2/(1 + n)^2]$,[25] which is less than $\pi\alpha/n$, the transmission through the graphene electrode on a substrate is significantly lower than that of either the bare graphene structure or the optical impedance transformer structure.

We now consider the angular response. An ideal optical impedance transformer should be able to reduce the impedance of the electromagnetic wave incident upon the electrode without any reflection for any angle of incidence. With an ideal optical impedance transformer, the transmission through the structure including the transparent conducting electrode layer is

$$T_s = 1 - \pi\alpha\frac{N}{n}\frac{1}{\cos\varphi} \tag{7}$$

for the s-polarization and

$$T_p = 1 - \pi\alpha\frac{N}{n}\left[\cos\varphi - \left(\frac{n^2}{|\tilde{\varepsilon}|}\right)^2\frac{\sin^2\varphi}{\cos\varphi}\right] \tag{8}$$

for the p-polarization, where φ is related to the incident angle θ by Snell's law $\sin\theta = n\sin\varphi$ and $\tilde{\varepsilon}$ is the relative complex dielectric constant of graphene. Equations 7 and 8 define the red dashed curves in Figure 3.

For our structure in Figure 1, we simulate its off-normal incidence for both s- and p-polarizations, when light with its parallel wavevector along the [10] direction of the lattice is incident upon the structure. We see that our structure behaves very close to an ideal optical impedance transformer over a very large angular range for both polarizations. For the s-polarization, the structure in Figure 1 has a transmission above 97% for an angle of incidence up to 60°. This structure also has a higher transmission over all angles of incidence, as compared to graphene layers either suspended in air, or put on the top surface of a structure (Figure 3a). For the p-polarization, the transmission of the structure in Figure 1 is over 97% for an angle of incidence up to 40°. It also outperforms both planar structures in transmission up to 40° (Figure 3b). Further optimization of the nanostructures is likely to slightly improve the performance.

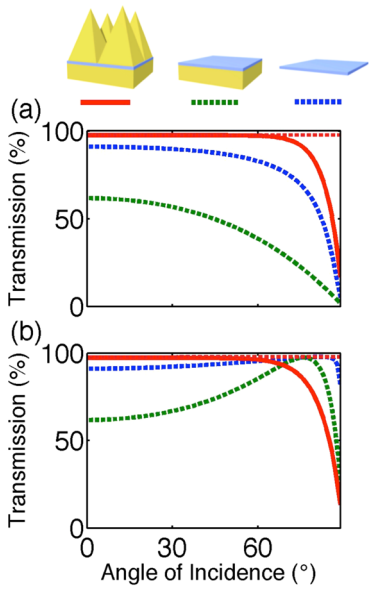

Figure 3. Comparison of spectrally averaged transmission coefficients of the (a) s- and (b) p-polarization for the same structures in Figure 2. The blue curves correspond to the bare graphene layers, the green curves correspond to the graphene layers on the substrate, and the red curves correspond to the structure with optical impedance transformation. The dashed red curves correspond to ideal optical impedance transformers as defined by eqs 7 and 8

In practice, the angular average of the optical properties is important. For example, in nontracking solar cells, and also because a significant portion of the sunlight is diffusive, the relevant quantity is the angular average of the transmission according to the formula $\overline{T} = \int d\theta\ T(\theta)\cos\theta$. The angular, spectral, and polarization averaged transmission of the 4-layer graphene in air is 90%, and this averaged transmission is improved to 96.4% with the optical impedance transformer.

The concept of optical impedance transformation applies well to other numerical values of the refractive indices of the materials, as well as to other thicknesses of the ultrathin film. In Figure 4, we plot the simulated transmission coefficients at normal incidence at 500 nm for a wide range of structures like Figure 1. For each N and n, we have chosen a locally optimal set of values of l and h. The simulation results agree with the theoretical predictions given by eq 6. In the visible wavelength range, with Ta_2O_5 (n = 2.1) as the surrounding medium, for example, one could reduce the optical loss of a graphene electrode by 50%. For thin transparent conducting electrode with thickness beyond approximately 3 nm, the optimized structure outperforms the predicted transmission (Figure 4b). The structure in Figure 1 is in fact useful for any transparent conducting electrode with subwavelength thickness. The effectiveness of our strategy to suppress absorption and to enhance transmission in any subwavelength transparent conducting electrode can be derived analytically with boundary condition matching.

Finally, we remark that the concept of impedance transformation as a mechanism for loss reduction is certainly well-known at lower frequencies. For electric power transmission, for a given power that needs to be transmitted one routinely uses transformers to increase the voltage and reduce the current in order to reduce the power dissipation in the transmission

dx.doi.org/10.1021/nl500741f | Nano Lett. 2014, 14, 2755−2758

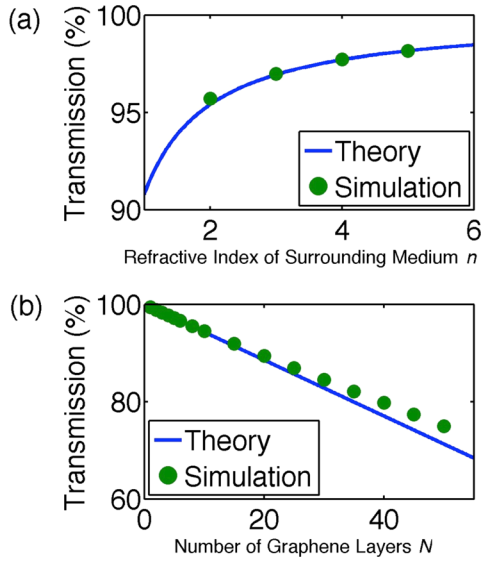

Figure 4. Transmission coefficients of normally incident light with a wavelength of 500 nm on the optical impedance transformer structure. The continuous curves are theoretical predictions by eq 6. Each discrete data point corresponds to a simulated structure in Figure 1 with optimal l and h. (a) Transmission coefficients with different refractive indices n of surrounding medium and N = 4. (b) Transmission coefficients with different numbers N of graphene layers and n = 4.

lines. In the optical regime, previous works have also used the concept of impedance to describe plasmonic circuits[26,27] and the concept of impedance transformation to achieve deep-subwavelength optical confinements.[28] Our work is analogous to the electric transformer concepts at lower frequencies. The original contribution here is the realization that the concept of optical impedance transformation can be used to reduce the loss of a transparent conducting electrode without influencing its electrical properties, and the two key ingredients are impedance matching for improved transmission and local electric field modification for suppressed absorption. As we have shown in the paper, this concept results in a robust, broadband and omnidirectional reduction of the optical loss in a transparent electrode and therefore can be used to bypass the electric-optical trade-off that has been commonly considered as a fundamental constraint in transparent electrode design.

AUTHOR INFORMATION

Corresponding Author

*E-mail: shanhui@stanford.edu.

Notes

The authors declare no competing financial interest.

ACKNOWLEDGMENTS

The authors acknowledge discussions with the Fan group and Zhenan Bao. This work is supported by the Bay Area Photovoltaic Consortium (BAPVC) funded under the Sunshot Initiative of U.S. Department of Energy, by the Center on Nanostructuring for Efficient Energy Conversion (CNEEC) at Stanford University, an Energy Frontier Research Center funded by the U.S. Department of Energy, Office of Science and Office of Basic Energy Sciences under award number DE-SC0001060, and by the Department of Energy Grant DE-FG07ER46426. The simulations were performed on the Extreme Science and Engineering Discovery Environment (XSEDE), which is supported by National Science Foundation Grant OCI-1053575. J.R.P. also acknowledges the support of a Stanford Graduate Fellowship.

REFERENCES

(1) Wang, X.; Zhi, L.; Müllen, K. *Nano Lett.* **2008**, *8*, 323−327.
(2) Jo, G.; Choe, M.; Cho, C.-Y.; Kim, J. H.; Park, W.; Lee, S.; Hong, W.-K.; Kim, T.-W.; Park, S.-J.; Hong, B. H.; Kahng, Y. H.; Lee, T. *Nanotechnology* **2010**, *21*, 175201.
(3) Bae, S.; et al. *Nat. Nanotechnol.* **2010**, *5*, 574−578.
(4) Kang, J.; Kim, H.; Kim, K. S.; Lee, S.-K.; Bae, S.; Ahn, J.-H.; Kim, Y.-J.; Choi, J.-B.; Hong, B. H. *Nano Lett.* **2011**, *11*, 5154−5158.
(5) Kim, H.; Gilmore, C. M.; Piqué, A.; Horwitz, J. S.; Mattoussi, H.; Murata, H.; Kafafi, Z. H.; Chrisey, D. B. *J. Appl. Phys.* **1999**, *86*, 6451.
(6) Minami, T. *Semicond. Sci. Technol.* **2005**, *20*, S35−S44.
(7) Catrysse, P. B.; Fan, S. *Nano Lett.* **2010**, *10*, 2944−2949.
(8) Diamond, A. M.; Corbellini, L.; Balasubramaniam, K. R.; Chen, S.; Wang, S.; Matthews, T. S.; Wang, L.-W.; Ramesh, R.; Ager, J. W. *Phys. Status Solidi A* **2012**, *209*, 2101−2107.
(9) Wu, H.; Kong, D.; Ruan, Z.; Hsu, P.-C.; Wang, S.; Yu, Z.; Carney, T. J.; Hu, L.; Fan, S.; Cui, Y. *Nat. Nanotechnol.* **2013**, *8*, 421.
(10) Tolstoy, V. P.; Chernyshova, I. V.; Skryshevsky, V. A. *Handbook of Infrared Spectroscopy of Ultrathin Films*; John Wiley & Sons, Inc.: New York, 2003.
(11) Hägglund, C.; Apell, S. P.; Kasemo, B. *Nano Lett.* **2010**, *10*, 3135−3141.
(12) Zhu, J.; Yu, Z.; Fan, S.; Cui, Y. *Mater. Sci. Eng. R* **2010**, *70*, 330−340.
(13) Raut, H. K.; Ganesh, V. A.; Nair, A. S.; Ramakrishna, S. *Energy Environ. Sci.* **2011**, *4*, 3779.
(14) Wang, K. X.; Yu, Z.; Liu, V.; Cui, Y.; Fan, S. *Nano Lett.* **2012**, *12*, 1616−1619.
(15) Bonaccorso, F.; Sun, Z.; Hasan, T.; Ferrari, A. C. *Nat. Photonics* **2010**, *4*, 611−622.
(16) Gu, T.; Petrone, N.; McMillan, J. F.; van der Zande, A.; Yu, M.; Lo, G. Q.; Kwong, D. L.; Hone, J.; Wong, C. W. *Nat. Photonics* **2012**, *6*, 554−559.
(17) Xia, F.; Yan, H.; Avouris, P. *Proc. IEEE* **2013**, *101*, 1717−1731.
(18) Liu, M.; Zhang, X. *Nat. Photonics* **2013**, *7*, 851−852.
(19) Butler, S. Z.; et al. *ACS Nano* **2013**, *7*, 2898−2926.
(20) Nair, R. R.; Blake, P.; Grigorenko, A. N.; Novoselov, K. S.; Booth, T. J.; Stauber, T.; Peres, N. M. R.; Geim, A. K. *Science* **2008**, *320*, 1308.
(21) Mak, K. F.; Ju, L.; Wang, F.; Heinz, T. F. *Solid State Commun.* **2012**, *152*, 1341−1349.
(22) Bruna, M.; Borini, S. *Appl. Phys. Lett.* **2009**, *94*, 031901.
(23) Liu, V.; Fan, S. *Comput. Phys. Commun.* **2012**, *183*, 2233−2244.
(24) Wu, J.; Becerril, H. A.; Bao, Z.; Liu, Z.; Chen, Y.; Peumans, P. *Appl. Phys. Lett.* **2008**, *92*, 263302.
(25) Fang, H.; Bechtel, H. A.; Plis, E.; Martin, M. C.; Krishna, S.; Yablonovitch, E.; Javey, A. *Proc. Natl. Acad. Sci. U.S.A.* **2013**, *110*, 11688−11691.
(26) Veronis, G.; Fan, S. *Appl. Phys. Lett.* **2005**, *87*, 131102.
(27) Staffaroni, M.; Conway, J.; Vedantam, S.; Tang, J.; Yablonovitch, E. *Phot. Nanostruct. Fundam. Appl.* **2012**, *10*, 166−176.
(28) Choo, H.; Kim, M.-K.; Stafarroni, M.; Seok, T. J.; Bokor, J.; Cabrini, S.; Schuck, P. J.; Wu, M. C.; Yablonovitch, E. *Nat. Photonics* **2012**, *6*, 838−844.